A preclinical algorithm of soluble surrogate biomarkers that correlate with therapeutic inhibition of the MET oncogene in gastric tumors.

A preclinical algorithm of soluble surrogate biomarkers that correlate with therapeutic inhibition of the MET oncogene in gastric tumors†

Davide Torti[1], Francesco Sassi[1],Francesco Galimi[1], Stefania Gastaldi[1],Timothy Perera[2], Paolo M. Comoglio[1,‡,*],Livio Trusolino[1,§,¶,*] andAndrea Bertotti[1,¶]

Author Information

[1]Laboratory of Molecular Pharmacology, Institute for Cancer Research and Treatment (IRCC), University of Torino Medical School, Candiolo, Torino, Italy

[2]Cancer Biology Oncology Discovery, Janssen Research and Development, Beerse, Belgium

[¶]L.T. and A.B. contributed equally to this work as senior authors.

[‡]Tel: +39-011-993.3202, Fax: +39-011-993.3225

[§]Tel: +39-011-993.3202, Fax: +39-011-993.3225

Email: Paolo M. Comoglio (pcomoglio@gmail.com), Livio Trusolino (livio.trusolino@ircc.it)

[*]Division of Molecular Oncology, IRCC, Institute for Cancer Research and Treatment, University of Torino Medical School, Strada Provinciale 142, km 3.95, 10060 Candiolo, Torino, Italy

[†]Conflict of interest: TP is a full-time employee of Janssen pharmaceutical companies of Johnson & Johnson. PMC receives research grants from Janssen pharmaceutical companies

Funded by
European Union Seventh Framework Programme FP7/2007-2011. Grant Numbers: 201279, 201640
AIRC. Grant Number: 9970
AIRC. Grant Numbers: 4682, 10116
MIUR (Ministero dell'Università e della Ricerca)
MIUR FIRB (Fondo per gli Investimenti della Ricerca di Base)—Futuro in Ricerca
FPRC (Fondazione Piemontese per la Ricerca sul Cancro)

ABSTRACT

The MET oncogene is amplified in a fraction of human gastric carcinoma cell lines, with consequent overexpression and constitutive activation of the corresponding protein product, the Met tyrosine kinase receptor. This genetically driven hyperactivation of Met is necessary for cancer cell growth and survival, so that Met pharmacological blockade results in cell-cycle arrest or apoptosis (oncogene addiction). MET gene amplification also occurs *in vivo* in a number of human gastric carcinomas, and clinical trials are now ongoing to assess the therapeutic efficacy of Met inhibitors in this type of malignancy. The aim of our study was to identify a preclinical algorithm of soluble surrogate biomarkers indicative of response to Met inhibition in gastric tumors, as a potential tool to integrate imaging criteria during patient follow-up. We started from a survey of candidate molecules based on antibody proteomics and gene expression profiling; after ELISA validation and analytical quantification, four biomarkers were identified that appeared to be strongly and consistently modulated by Met inhibition in a panel of Met-addicted gastric carcinoma cell lines, but not in Met-independent cell lines. Pharmacologic blockade of Met using specific small-molecule inhibitors led to reduced secretion of IL-8, GROα and the soluble form of uPAR and to increased production of IL-6 both *in vitro* (in culture supernatants) and *in vivo* (in the plasma of xenografted mice). If confirmed in patients, this information might prove useful to monitor clinical response to Met-targeted therapies in MET-amplified gastric carcinomas.

Keywords: targeted therapies; Met receptor; surrogate biomarkers; oncogene addiction

Gastric cancer is the fourth most common malignancy in the world and the first leading cause of cancer deaths in Asia. Notwithstanding the advancement of surgical techniques and the introduction of new chemotherapeutic regimens, patients with advanced disease still face a dismal prognosis. As already observed for other solid tumors, the advent of targeted therapies against "druggable" oncoproteins is also likely to improve clinical outcome in the context of this specific malignancy.

The Met tyrosine kinase receptor for hepatocyte growth factor (HGF) is abnormally activated in a fraction of human gastric cancers; indeed, amplification of the MET gene has been reported in ~ 7% of unselected patients and in more than 38% of cases when considering tumors of the scirrhous type in the Japanese population.1–4 Consistent with these epidemiological findings, MET amplification is a genetic hallmark of several cultured cell lines derived from gastric tumors.4, 5 These MET-amplified gastric carcinoma cell lines respond to Met inactivation with remarkable growth impairment, suggesting that this kind of genetic alteration drives "addiction" to Met activity *in vitro* and may predict effective treatment outcome *in vivo*.4, 5 Such findings have encouraged the development of several anti-Met antibodies and small-molecule Met inhibitors, many of which are currently undergoing Phase I and Phase II clinical trials in different neoplastic settings, including gastric tumors.6–8

During patient follow-up, response to treatment is classically defined through repeated measurements of the tumor size by imaging techniques (which normally involve computed tomography and/or magnetic resonance). Thanks to its extensive application and informative value, this procedure has become the gold standard to assess the efficacy of anticancer therapies and is now a universally recognized criterion for response evaluation in solid tumors (RECIST).9 However, some practical and biological shortcomings undermine full reliability of this approach: consistency in pursuing the correct imaging requirements and rules in different centers worldwide is challenging; recurrent body irradiation raises important safety concerns, which imposes relatively long holding periods between one examination and the other and finally, because some tumors retain their original peripheral mass while showing a central core of necrotic or liquefied tissue, dimensional responses are not always correlated with the actual clinical benefit.10

Based on these considerations, there is now general agreement that imaging criteria should be integrated by other noninvasive methods allowing for dynamic, short-term and serial monitoring of tumor response to therapy.11 This would be particularly helpful in the assessment of the results of Phase I and II studies, in which critical decisions are made regarding the merits of continued investigation of a particular agent. One such method relies on the measurement of the plasma levels of soluble proteins shown to undergo rapid, objective and quantifiable changes in their blood concentration only when tumors are sensitive to a given anticancer therapy. Variations of these analytes must correlate with response to treatment but do not necessarily provide functional information; therefore, these soluble indicators are conventionally known as surrogate response biomarkers.12

Here, we addressed this issue by performing a preclinical exploratory study in the context of MET-amplified gastric tumors responsive to anti-Met-targeted therapies. Starting from a wide list of candidates selected from antibody-based proteomics and gene expression profiling, we finally extracted an algorithm of four soluble proteins that appeared to be consistently modulated by Met pharmacologic blockade in a panel of drug-sensitive gastric carcinoma cell lines. Specifically, Met inhibition led to reduced levels of IL-8, GROα and uPAR and to increased secretion of IL-6, both in culture supernatants and in the plasma of mice bearing gastric carcinoma xenografts. If validated in the clinic, such biomarkers might prove useful to supervise patient follow-up in association with conventional imaging.

MATERIALS AND METHODS

Cell lines and reagents

SNU5, HS746T, NCI-N87 and AGS were acquired from American Type Culture Collection; MKN45 was purchased from Riken Cell Bank; GTL16 is a subclone of MKN45 obtained by limiting dilution.13 GTL16, MKN45, NCI-N87 and AGS were maintained in RPMI 1640, SNU5 and HS746T in Iscove, both complemented with 10% fetal bovine serum, 4 mmol/l glutamine and antibiotics. PHA-665752 was purchased from Tocris Bioscience. For *in vivo* experiments, JNJ-38877605 was provided by Ortho Biotech Oncology. GTL16 cells expressing K-RAS^{G12V} have already been described.14

Protein arrays and densitometric analysis

A Human Cytokine Antibody Array kit was purchased from RayBiotech. Briefly, membranes were saturated with a blocking buffer, exposed to culture supernatants from GTL16 cells treated with either the Met small-molecule inhibitor PHA-665752 (PHA; 0.5 μM, 24 or 72 hr) or DMSO and incubated at room temperature for 2 hr. After incubation with primary biotin-conjugated antibody, membranes were developed using enhanced chemiluminescence-type solution (ECL, Amersham). Images were captured using a LAS-4000 molecular imager (Fujifilm). Densitometric analysis was performed with the MetaMorph® software, using region of interest integrated intensity function. Raw intensity values were background corrected by subtracting the average signal of blank spots and normalized using positive controls as references.

ELISA kits

STC2 ELISA kit was purchased from USCN Life Sciences; IL-6 and MIF ELISA kits were purchased from Bender MedSystems; all other kits were purchased from R&D. Experiments were performed according to the manufacturer's instructions.

Oligonucleotide microarrays and TaqMan low-density qPCR array

Total RNA was isolated with TRIzol (Invitrogen). Gene expression datasets, obtained by oligonucleotide microarrays, have already been published14 and have been deposited in the National Center for Biotechnology Information Gene Expression Omnibus (GEO;http://www.ncbi.nlm.nih.gov/geo/ under the GEO Series accession number GSE19043). For TaqMan low-density quantitative polymerase chain reaction (qPCR) array, cDNA was prepared using the High-Capacity cDNA Reverse Transcription Kit (Applied Biosystems). TaqMan qPCR reactions targeted 43 transcripts chosen among the top-ranking genes encoding secreted/soluble proteins, based on microarray expression profiles, and two reference genes (POL2AR and B2M) in a microfluidic card.

Viability assays

One thousand cells were resuspended in 50 μl of complete growth medium and seeded in 96-well plastic culture plates (Day 0). On Day 1, 50 μl of PHA-665752 or vehicle serially diluted in complete medium was added to cells. On Day 3, cell viability was assessed by ATP content using a luminescence assay (CellTiter-Glo, Promega). All measurements were recorded using a Victor™ X4 2030 multilabel plate reader (Perkin Elmer). Growth inhibition at each drug concentration was normalized to vehicle-treated cells.

Xenografts and *in vivo* procedures

GTL16 cells (2×10^6) were resuspended in 200 μl of PBS and inoculated subcutaneously into the right posterior flank (or both right and left posterior flanks, for determination of uPAR and IL-6) of 6-

week-old immunodeficient *nu/nu* female mice on Swiss CD1 background (Charles River Laboratories). After tumor mass formation, mice were dosed orally with 40 mg/kg/day of the Met inhibitor JNJ-38877605 for 3 days. Blood was sampled from tail vein or heart at the indicated timepoints, and plasma was assayed for the concentration of the selected analytes by ELISA. All animal procedures were approved by the Ethical Commission of the Institute for Cancer Research and Treatment (Candiolo, Torino, Italy) and by the Italian Ministry of Health.

Statistics

Results are means ± standard error of the means (SEM) for both *in vitro* and *in vivo* experiments. When applicable, comparisons were made using the two-tailed Student's *t*-test. *p* values less than 0.05 were considered to be statistically significant.

RESULTS

A multiplatform screen identifies candidate soluble biomarkers of Met inhibition

To explore the “secretome” of drug-sensitive cancer cells in response to Met inhibition, we devised a sequential experimental pipeline that incorporated different multiplex technologies in a number of MET-amplified, Met-addicted cell lines (Fig. 1*a*). First, we undertook a medium-scale screen using a highly sensitive, membrane-based protein array system that enabled simultaneous detection of 120 cytokines and soluble molecules in a simple dot-plot format, using cell culture supernatants as a source of analytes. This platform was expanded with data derived from a large-scale, genome-wide expression profiling study. Both the proteomic screen and the genome-wide transcriptional analysis were performed in the gastric carcinoma cell line GTL16, which contains 11 extra copies of the MET locus and undergoes a complete proliferative arrest upon Met inhibition.14, 15 PHA-665752 (subsequently referred to as PHA), a well-characterized Met-specific inhibitor,16was chosen for Met pharmacologic blockade.

For antibody-based proteomics, data were collected by probing the membranes with GTL16 cell culture supernatants after two different timepoints, 24 and 72 hr, in the presence or absence of 0.5 μM PHA (Fig. 1*b*). Inhibition of Met-dependent signals is known to induce a marked decrease in the proliferation rate of fast-growing Met-addicted cells.4, 5, 14, 16 This would likely bias the quantitative assessment of functional changes in the amount of secreted proteins, due to reduction in the absolute number of cells as a consequence of Met neutralization. We were able to overcome this limitation by administering PHA after cell overconfluency: under this condition, cells achieve a growth plateau that is not affected by the proliferative arrest induced by Met inhibition.14 Computer-assisted densitometry of the arrayed spots was performed to quantitate differences in the amounts of secreted molecules: ten proteins, which exhibited a positive or negative modulation greater than twofold following PHA treatment, were scored as hits (Fig. 1*c*). The temporal trends of changes in protein secretion appeared to be quite variable: growth-related oncogene α (GROα), interleukin-8 (IL-8) and insulin-like growth factor binding protein 1 (IGFBP-1) displayed early changes, with negative modulation after 24 hr of Met inhibition; the soluble forms of interleukin-6 receptor (IL-6R), plasminogen activator urokinase receptor (uPAR or PLAUR), tumor necrosis factor receptor superfamily member 1B (STNFR2) and tumor necrosis factor receptor superfamily member 11B (OPG or TNFSR11B) had a delayed pattern, with decreased production mainly at 72 hr. The modulation of chemokine (C-C motif) ligand 2 (MCP-1 or CCL2) and interleukin-6 (IL-6) had an opposite direction, with marked protein accumulation after 72 hr of Met inhibition. Finally, secretion of TIMP metallopeptidase inhibitor 2 (TIMP2) exhibited a bimodal dynamics: the molecule was upregulated after 24 hr of Met inhibition and downregulated after 72 hr.

For unbiased gene expression analysis, we took advantage from a transcriptional portrait of GTL16 cells treated for 24 hr with 1 μM PHA, previously generated through oligonucleotide microarray technology.14 From this dataset, we extracted ~ 1,000 secreted/soluble proteins using publicly available bioinformatic tools (Gene Ontology and Secreted Protein Database; http://spd.cbi.pku.edu.cn) and identified those transcripts that proved to be modulated by Met inhibition. Then, the 43 top-ranking molecules featuring the highest extents of transcriptional modulation were reassessed for expression changes by TaqMan low-density qPCR arrays. This validation step was carried out in GTL16 cells and further extended to a panel of three other gastric carcinoma cell lines (MKN45, HS746T and SNU5), all exhibiting amplification of the MET oncogene and responding to Met inhibition with a severe impairment of cell viability4, 5, 14 (Fig. 1*a*). For selection of candidates, we considered the modulation of all 43 transcripts across the four cell lines and concentrated on the genes that concordantly displayed decreased or increased expression (following Met inhibition) with an average $\log_2$ ratio greater than ±2 (Fig. 1*d*). Among such genes, uPAR and IL-8 were confirmed to be downregulated in GTL16 and to undergo robust downregulation also in MKN45, HS746T and SNU5. Other molecules that were not interrogated in our initial proteomic approach demonstrated coherent expression changes across the entire panel of Met-addicted cell lines: these included one molecule that was consistently upregulated upon Met inhibition (macrophage stimulating 1, MST1) and six molecules that were downregulated (bone morphogenetic protein 6, BMP6; galanin, GAL; stanniocalcin 2, STC2; endothelial lipase, LIPG; uridine phosphorylase 1, UPP1 and regenerating islet-derived family, member 4, REG4) (Fig. 1*d*).

In short, a sequential, complementary and multiplatform screen allowed the identification of ten soluble molecules that proved to be modulated in response to Met inhibition in GTL16 (as assessed by protein arrays) and nine genes encoding for secreted molecules whose expression consistently changed upon Met inhibition in a panel of four Met-addicted gastric carcinoma cell lines (as assessed by TaqMan-based qPCR low-density arrays). Of these, two (IL-8 and uPAR) were concomitantly interrogated by both proteomic and transcriptional analyses (Fig. 1*a*). For further validation and absolute quantification of changes in secretion in the whole Met-addicted cell panel, we selected eight candidates for which commercial ELISA assay kits were available: IL-8, uPAR, GROα, MCP-1, IL-6, GAL, STC2 and REG4.

Met inhibition induces consistent changes in the secretion of IL-8, uPAR, GROα and IL-6 in a panel of Met-addicted gastric carcinoma cell lines

We quantitated the changes in protein concentration of the candidate molecules in the culture supernatants of Met-addicted cell lines, following Met pharmacological blockade in overconfluent cells. Cells were exposed to DMSO or 0.5 μM PHA for 24 hr (IL-8, GROα, GAL, STC2 and REG4) or 72 hr (uPAR, IL-6 and MCP-1), in accordance with the timepoint of maximal modulation observed in the screening experiments; supernatants were then collected and tested with the appropriate ELISA kit assays. As already mentioned, inhibition of Met in overconfluent Met-addicted cell lines did not substantially affect cell growth, thus avoiding the confounding contribution of cell number variations to the production of the secreted molecules (Supporting Information Fig. 1).

Consistent with the previous results, we measured a statistically significant decrease in the concentrations of IL-8, GROα and uPAR in supernatants derived from the four addicted cell lines treated with PHA (Figs. 2*a*–2*c*) as well as a robust increase of IL-6 production in PHA-inhibited GTL16, MKN45 and HS746 (Fig. 2*d*). SNU5 cells were an exception, as both basal and PHA-modulated levels of IL-6 were under the detection threshold. Similarly, both basal and PHA-induced amounts of the other four molecules tested (MCP-1, GAL, STC2 and REG4) were below the detectable protein concentration range of the corresponding ELISA kits. Cell lines displayed

remarkable differences in the physiological secretion of the investigated proteins: for instance, the basal concentration of IL-8 in GTL16 amounted to ~ 0.250 ng/ml, whereas it was above 13 ng/ml in SNU5 cells (Fig. 2*a*). Notwithstanding these differences in absolute production levels, Met inhibition invariably induced a clearcut modulation of their secreted quantities.

Collectively, these results confirm and quantitate the magnitude of the modulation trend observed at the proteomic and transcriptional levels for IL-8, GROα, uPAR and IL-6. Furthermore, the feasibility of protein detection through quantitative analytical methods affords these four molecules with additional preclinical value as potential serum biomarkers of Met inhibition.

Modulation of IL-8, uPAR, GROa and IL-6 is blunted in cells that are biologically insensitive to Met inhibition

In principle, changes in the secretion of IL-8, GROα, uPAR and IL-6 by Met-addicted gastric carcinoma cells could be due to blockade of Met activity independent of the therapeutic response. In this case, the algorithm would correlate with Met pharmacologic inhibition but not with reduction of tumor cell growth. To address this issue, we assayed the concentrations of IL-8, GROα, uPAR and IL-6 in the supernatants of different cellular models of therapeutic resistance to Met inhibition. In the first model, we rendered Met-addicted GTL16 cells unresponsive to Met inhibition by exogenous expression of a constitutively active form of Ras (Ras^{G12V}): we have already demonstrated that, in this setting, treatment with Met inhibitors leads to biochemical inactivation of Met, but it does not induce cell-cycle arrest.14 In $GTL16^{RasG12V}$, the decrease in the production of IL-8, GROα and uPAR induced by PHA treatment was much lower than that observed in wild-type GTL16 (approximately twofold in $GTL16^{RasG12V}$ *versus* approximately eightfold in wild-type GTL16). Similarly, IL-6 levels remained under the detection threshold in $GTL16^{RasG12V}$ cells both in the absence and in the presence of Met inhibition, whereas the concentration of IL-6 reached the detection range in Met-inhibited wild-type GTL16 (indicative of enhanced secretion) (Fig. 3*a*).

The other models included two additional gastric carcinoma cell lines, NCI-N87 and AGS, which express physiological levels of Met17(Supporting Information Fig. 2*a*). According to quantitative assessment of Met phosphorylation levels by ELISA assays, HGF treatment (50 ng/ml) was able to induce activation of Met in both NCI-N87 and AGS, and in both cell lines administration of 0.5 μM PHA abrogated HGF-induced Met phosphorylation (Supporting Information Fig. 2*b*). Viability assays of cells cultured in the presence of HGF and treated with increasing concentrations of PHA revealed that Met blockade did not affect cell growth (Supporting Information Fig. 2*c*). This indicates that, similar to the $GTL16^{RasG12V}$ setting, NCI-N87 and AGS respond to Met inhibitors with receptor dephosphorylation, but not with growth suppression. Again in analogy with $GTL16^{RasG12V}$, production of IL-8, GROα and uPAR in these cell lines was not influenced by Met inhibition, and IL-6 levels remained undetectable both in the absence and in the presence of PHA (Fig. 3*b*).
Together, these data indicate that changes in the secretion of the four biomarkers are negligible—if any—in cells in which inhibition of constitutive or HGF-induced Met activation is not accompanied by a proliferative impairment, whereas production of such molecules is profoundly affected in Met-addicted cell lines that respond to Met inhibition with a severe growth arrest. When translated into the clinical setting, this observation suggests that serum positivity for this algorithm may predict both target inhibition and actual therapeutic response.

Pharmacological inhibition of Met-addicted xenografts induces consistent changes in plasma concentration of IL-8, GROa, uPAR and IL-6

To further validate the preclinical significance of these results, we extended our analysis to an *in vivo* model of tumor xenotransplantation. Specifically, we inoculated GTL16 cells in

immunocompromised mice and let the xenografts grow until formation of established tumor masses (range of tumor volumes between 800 and 1,200 mm^3). We then treated the mice with JNJ-38877605, another Met small-molecule inhibitor that—different from PHA—displays oral bioavailability and is endowed with a safer *in vivo* toxicity profile.6, 18*In vitro* experiments demonstrated that JNJ-38877605 is as efficient as PHA in modulating secretion of the investigated molecules in GTL16 cells (Supporting Information Fig. 3).

Preliminary findings in untreated mice bearing established GTL16 xenografts indicated that the basal plasma levels of tumor-derived human IL-8 and GROα fell in the range of analytical detectability, whereas those of uPAR and IL-6 were below quantification limits. Therefore, we decided to proceed with two different experimental approaches. In the case of IL-8 (n = 6) and GROα (n = 4), mice were dosed orally with 40 mg/kg JNJ-38877605 once daily for 3 days, and blood was sampled sequentially from the tail vein of each mouse immediately before treatment initiation (timepoint 0) and after completion (timepoint 72 hr). In the case of uPAR and IL-6, we reasoned that one way to increase plasmatic detectability was to maximize tumor masses—in order to boost the amount of secreted proteins—and to dispose of higher volumes of blood. Accordingly, we inoculated cells on both flanks of each mouse and took blood samples directly from the heart of sacrificed animals, which allowed separation of higher quantities of plasma. To do this, we produced independent experimental groups for untreated and treated animals, which were matched by similar tumor volumes (n = 6 for uPAR and 4 for IL-6).

Treatment of mice with JNJ-38877605 for 72 hr led to a statistically significant decrease in the plasma levels of human IL-8 (from ~ 0.150 to 0.050 ng/ml) and GROα (from 0.080 to 0.030 ng/ml) (Fig. 4). The blood concentration of uPAR also diminished by more than 50% (Fig. 4). While confirming the trend observed *in vitro*, the extent of uPAR reduction induced by Met inhibition *in vivo* was extremely variable among the different mice and did not reach statistical significance; this is possibly due to the fact that, in this specific experimental setting, samples from independent animals instead of paired samples were examined (see above). Consistent with the results obtained *in vitro*, systemic inhibition of Met resulted in an increase of IL-6 from underthreshold levels to a detectable amount of ~ 0.015 ng/ml (Fig. 4).

DISCUSSION

Unlike biopsies, plasma proteins can be serially measured easily and noninvasively, allowing one to assess, in a short period, whether changes in their blood concentration can correlate with defined clinical (and, possibly, functional) responses. Prompted by the notion that soluble biomarkers should be investigated as complementary instruments to monitor tumor responses, especially when investigational targeted therapies move from the preclinical setting to first-in-man studies, we decided to undertake a top-down exploratory study of secreted molecules whose expression is modulated by Met inhibition in MET-amplified gastric carcinoma cell lines. These cells respond to Met pharmacologic inhibition with drastic growth impairment, a finding that has spurred the design of *ad hoc* clinical trials to evaluate whether Met inhibitors can have therapeutic efficacy in MET-amplified gastric tumors.4–8, 14, 16

Starting from an antibody-based proteomic survey and a gene ontology annotation of secreted molecules extracted from a genome-wide expression dataset, we selected some candidates that were validated in a panel of “Met-addicted” cellular models of gastric cancer origin. Through this experimental pipeline, we ended up with four soluble biomarkers (IL-8, GROα, uPAR and IL-6) whose secretion was consistently and significantly modulated in all the cell lines tested. At least in part, this algorithm may also apply to tumor settings other than gastric carcinoma: preliminary results in two MET-amplified, Met-addicted lung cancer cell lines reveal an analogous trend of

protein modulation for IL-8, GROα and uPAR, whereas IL-6 appears to be downregulated rather than upregulated (Supporting Information Fig. 4).

Because these molecules are related to broad systemic parameters such as inflammation and coagulation, we expect that baseline levels for each of them will exhibit interindividual variability when tested in humans. However, it is worth noting that the circulating levels of the four cytokines have already been assayed (and found to be increased) in a variety of tumor patients, including, in the case of IL-8 and IL-6, gastric carcinoma patients.19–22 These results indicate that the analytical determination of such biomarkers in human plasma is feasible and that their detectability in tumor patients appears not to be critically affected by physiological intersubject and within-subject variations. Therefore, if therapy-induced changes in the plasma concentration of the four biomarkers prove to be sufficiently robust for all of them, generation of a reliable and specific response algorithm can be realistically envisioned.

Another aspect that deserves consideration concerns the finding that these soluble proteins are not simply indicative of target impact, but they also correlate with tumor response: in cellular models of therapeutic resistance to Met inhibition, in which treatment with Met inhibitors results in Met deactivation but not in cell-cycle arrest,14 production of the biomarkers was only slightly affected. This allows discriminating between pharmacologic *versus* biological compound activity.

Changes in the expression of these secreted molecules might produce functional effects that transcend their activity as surrogate biomarkers. IL-8 and GROα share common structural features, similar receptors and superimposable roles.23 Both cytokines are transcriptionally upregulated by Ras-dependent signals, which are the major transducers of Met-driven growth in Met-addicted cancer cells.14, 24, 25 They are involved in the progression of different types of tumors by stimulating angiogenesis and inflammatory reactions within the tumor reactive microenvironment26–28 as well as proliferation, migration and survival of neoplastic cells.29–34 Moreover, they induce senescence of cancer-associated fibroblasts, which exacerbates the malignant properties of transformed cells.24, 25 Analogous biological properties are displayed by uPAR: both membrane-bound and serum-soluble forms of this receptor have been implicated in tumor angiogenesis,35 and increased levels of uPAR correlate with a poor prognosis and unfavorable clinical outcome in several neoplasms.36, 37 Accordingly, uPAR neutralization by antisense oligonucleotides or peptide antagonists prevents cancer growth, invasiveness and metastasis.38–40 All these observations suggest that reduction in the production of these proteins, such as that caused by Met inactivation, would lead to a depletion of proangiogenic and proinvasive cues; in turn, this adverse microenvironmental condition would likely cooperate with direct Met inhibition to promote tumor regression. Rather than being reduced, production of IL-6 is instead enhanced by Met blockade; in this context, it is noteworthy that IL-6 can exert an antiproliferative effect in oncogenically stressed cancer cells,41 which again might add on the growth impairment induced by Met pharmacologic inhibition *per se*.

In conclusion, we have identified a “secretomic” signature that correlates with drug sensitivity in Met-addicted gastric carcinomas and that might be mechanistically linked to tumor shrinkage as a consequence of Met inhibition. In our opinion, such biomarkers warrant prospective validation in clinical trials as applicative tools for frequent and noninvasive assessment of tumor response during patient follow-up.

Acknowledgements

The authors thank Laura Tarditi, Tuti Werdiningsih and Fabrizio Maina for animal care; Raffaella Albano, Stefania Giove and Laura Palmas for technical assistance and Antonella Cignetto for secretarial assistance. Work in the authors' laboratory is supported by grants from Johnson & Johnson and European Union Seventh Framework Programme FP7/2007-2011 to P.M.C.; AIRC

(Associazione Italiana per la Ricerca sul Cancro)—2010 Special Program Molecular Clinical Oncology 5 x 1000 to P.M.C. and L.T.; AIRC Investigator Grants to P.M.C. and L.T.; Regione Piemonte to P.M.C. and L.T.; MIUR (Ministero dell'Università e della Ricerca) to P.M.C.; MIUR FIRB (Fondo per gli Investimenti della Ricerca di Base)—Futuro in Ricerca to A.B. and FPRC (Fondazione Piemontese per la Ricerca sul Cancro) to L.T.

REFERENCES

1. Houldsworth J, Cordon-Cardo C, Ladanyi M, Kelsen DP, Chaganti RS. Gene amplification in gastric and esophageal adenocarcinomas. *Cancer Res* 1990; 50: 6417–22.

2. Kuniyasu H, Yasui W, Kitadai Y, Yokozaki H, Ito H, Tahara E. Frequent amplification of the c-met gene in scirrhous type stomach cancer. *Biochem Biophys Res Commun* 1992; 189: 227–32.

3. Hara T, Ooi A, Kobayashi M, Mai M, Yanagihara K, Nakanishi I. Amplification of c-myc, K-sam, and c-met in gastric cancers: detection by fluorescence in situ hybridization. *Lab Invest* 1998; 78: 1143–53.

4. Smolen GA, Sordella R, Muir B, Mohapatra G, Barmettler A, Archibald H, Kim WJ, Okimoto RA, Bell DW, Sgroi DC, Christensen JG,Settleman J, et al. Amplification of MET may identify a subset of cancers with extreme sensitivity to the selective tyrosine kinase inhibitor PHA-665752. *Proc Natl Acad Sci USA* 2006; 103: 2316–21.

5. McDermott U, Sharma SV, Dowell L, Greninger P, Montagut C, Lamb J, Archibald H, Raudales R, Tam A, Lee D, Rothenberg SM,Supko JG, et al. Identification of genotype-correlated sensitivity to selective kinase inhibitors by using high-throughput tumor cell line profiling. *Proc Natl Acad Sci USA* 2007; 104: 19936–41.

6. Comoglio PM, Giordano S, Trusolino L. Drug development of MET inhibitors: targeting oncogene addiction and expedience. *Nat Rev Drug Discov* 2008; 7: 504–16.

7. Trusolino L, Bertotti A, Comoglio PM. Met signalling: principles and functions in development, organ regeneration and cancer. *Nat Rev Mol Cell Biol* 2010; 11: 834–48.

8. http://clinicaltrials.gov/ct2/results?term=met+AND+gastric.

9. Therasse P, Arbuck SG, Eisenhauer EA. New guidelines to evaluate the response to treatment in solid tumors. *J Natl Cancer Inst*2000; 92: 205–16.

10. Desar IM, van Herpen CM, van Laarhoven HW, Barentsz JO, Oyen WJ, van der Graaf WT. Beyond RECIST: molecular and functional imaging techniques for evaluation of response to targeted therapy. *Cancer Treat Rev* 2009; 35: 309–21.

11. Sawyers CL. The cancer biomarker problem. *Nature* 2008; 452: 548–52.

12. Duivenvoorden R, de Groot E, Stroes ES, Kastelein JJ. Surrogate markers in clinical trials—challenges and opportunities.*Atherosclerosis* 2009; 206: 8–16.

13. Giordano S, Di Renzo MF, Ferracini R, Chiadò-Piat L, Comoglio PM. p145, a protein with associated tyrosine kinase activity in a human gastric carcinoma cell line. *Mol Cell Biol* 1988; 8: 3510–17.

14. Bertotti A, Burbridge MF, Gastaldi S, Galimi F, Torti D, Medico E, Giordano S, Corso S, Rolland-Valognes G, Lockhart BP, Hickman JA, Comoglio PM, et al. Only a subset of Met-activated pathways are required to sustain oncogene addiction. *Sci Signal* 2009; 2:ra80.

15. Rege-Cambrin G, Scaravaglio P, Carozzi F, Giordano S, Ponzetto C, Comoglio PM, Saglio G. Karyotypic analysis of gastric carcinoma cell lines carrying an amplified c-met oncogene. *Cancer Genet Cytogenet* 1992; 64: 170–3.

16. Christensen JG, Schreck R, Burrows J, Kuruganti P, Chan E, Le P, Chen J, Wang X, Ruslim L, Blake R, Lipson KE, Ramphal J, et al.A selective small molecule inhibitor of c-Met kinase inhibits c-Met-dependent phenotypes in vitro and exhibits cytoreductive antitumor activity in vivo. *Cancer Res* 2003; 63: 7345–55.

17. Bertotti A, Bracco C, Girolami F, Torti D, Gastaldi S, Galimi F, Medico E, Elvin P, Comoglio PM, Trusolino L. Inhibition of Src impairs the growth of Met-addicted gastric tumors. *Clin Cancer Res* 2010; 16: 3933–43.
18. Perera T. Selective inhibition of Met kinase: JNJ38877605. Spring CTEP Early Drug Development Meeting, Rockville, MD, USA,2007.
19. Druzgal CH, Chen Z, Yeh NT, Thomas GR, Ondrey FG, Duffey DC, Vilela RJ, Ende K, McCullagh L, Rudy SF, Muir C, Herscher LL, et al. A pilot study of longitudinal serum cytokine and angiogenesis factor levels as markers of therapeutic response and survival in patients with head and neck squamous cell carcinoma. *Head Neck* 2005; 27: 771–84.
20. Macrì A, Versaci A, Loddo S, Scuderi G, Travagliante M, Trimarchi GD, Teti D, Famulari C. Serum levels of interleukin 1beta, interleukin 8 and tumour necrosis factor alpha as markers of gastric cancer. *Biomarkers* 2006; 11: 184–93.
21. Shariat SF, Roehrborn CG, McConnell JD, Park S, Alam N, Wheeler TM, Slawin KM. Association of the circulating levels of the urokinase system of plasminogen activation with the presence of prostate cancer and invasion, progression, and metastasis. *J Clin Oncol* 2007; 25: 349–55.
22. Ikeguchi M, Hatada T, Yamamoto M, Miyake T, Matsunaga T, Fukumoto Y, Yamada Y, Fukuda K, Saito H, Tatebe S. Serum interleukin-6 and -10 levels in patients with gastric cancer. *Gastric Cancer* 2009; 12: 95–100.
23. Waugh DJ, Wilson C. The interleukin-8 pathway in cancer. *Clin Cancer Res* 2008; 14: 6735–41.
24. Coppé JP, Patil CK, Rodier F, Sun Y, Muñoz DP, Goldstein J, Nelson PS, Desprez PY, Campisi J. Senescence-associated secretory phenotypes reveal cell-nonautonomous functions of oncogenic RAS and the p53 tumor suppressor. *PLoS Biol* 2008; 6: 2853–68.
25. Yang G, Rosen DG, Zhang Z, Bast RC, Jr, Mills GB, Colacino JA, Mercado-Uribe I, Liu J. The chemokine growth-regulated oncogene 1 (Gro-1) links RAS signaling to the senescence of stromal fibroblasts and ovarian tumorigenesis. *Proc Natl Acad Sci USA*2006; 103: 16472–7.
26. Brat DJ, Bellail AC, Van Meir EG. The role of Interleukin-8 and its receptors in gliomagenesis and tumoral angiogenesis. *Neuro-oncology* 2005; 7: 122–33.
27. Li A, Dubey S, Varney ML, Dave BJ, Singh RK. IL-8 directly enhanced endothelial cell survival, proliferation, and matrix metalloproteinases production and regulated angiogenesis. *J Immunol* 2003; 170: 3369–76.
28. DeLarco JE, Wuertz BR, Furcht LT. The potential role of neutrophils in promoting the metastatic phenotype of tumors releasing interleukin-8. *Clin Cancer Res* 2004; 10: 4895–900.
29. Takamori H, Oades ZG, Hoch OC, Burger M, Schraufstatter IU. Autocrine growth effect of IL-8 and GROα on a human pancreatic cancer cell line, Capan-1. *Pancreas* 2000; 21: 52–6.
30. Brew R, Erikson JS, West DC, Kinsella AR, Slavin J, Christmas SE. Interleukin-8 as an autocrine growth factor for human colon carcinoma cells in vitro. *Cytokine* 2000; 12: 78–85.
31. Kamohara H, Takahashi M, Ishiko T, Ogawa M, Baba H. Induction of interleukin-8 (CXCL-8) by tumor necrosis factor-α and leukemia inhibitory factor in pancreatic carcinoma cells: impact of CXCL-8 as an autocrine growth factor. *Int J Oncol* 2007; 31: 627–32.
32. Yao C, Lin Y, Chua MS, Ye CS, Bi J, Li W, Zhu YF, Wang SM. Interleukin-8 modulates growth and invasiveness of estrogen receptor-negative breast cancer cells. *Int J Cancer* 2007; 121: 1949–57.
33. Araki S, Omori Y, Lyn D, Singh RK, Meinbach DM, Sandman Y, Lokeshwar VB, Lokeshwar BL. Interleukin-8 is a molecular determinant of androgen independence and progression in prostate cancer. *Cancer Res* 2007; 67: 6854–62.

34. Maxwell P, Gallagher R, Seaton A, Wilson C, Scullin P, Pettigrew J, Stratford IJ, Williams KJ, Johnston PG, Waugh DJ. HIF-1 and NF-κB-mediated upregulation of CXCR1 and CXCR2 expression promotes cell survival in hypoxic prostate cancer cells. *Oncogene*2007; 26: 7333–45.
35. Pepper MS. Role of the matrix metalloproteinase and plasminogen activator–plasmin systems in angiogenesis. *Arterioscler Thromb Vasc Biol* 2001; 21: 1104–17.
36. Stephens RW, Nielsen HJ, Christensen IJ, Thorlacius-Ussing O, Sørensen S, Danø K, Brünner N. Plasma urokinase receptor levels in patients with colorectal cancer: relationship to prognosis. *J Natl Cancer Inst* 1999; 91: 869–74.
37. Brünner N, Nielsen HJ, Hamers M, Christensen IJ, Thorlacius-Ussing O, Stephens RW. The urokinase plasminogen activator receptor in blood from healthy individuals and patients with cancer. *APMIS* 1999; 107: 160–7.
38. Lakka SS, Rajagopal R, Rajan MK, Mohan PM, Adachi Y, Dinh DH, Olivero WC, Gujrati M, Ali-Osman F, Roth JA, Yung WK, Kyritsis AP, et al. Adenovirus-mediated antisense urokinase-type plasminogen activator receptor gene transfer reduces tumor cell invasion and metastasis in non-small cell lung cancer cell lines. *Clin Cancer Res* 2001; 7: 1087–93.
39. Min HY, Doyle LV, Vitt CR, Zandonella CL, Stratton-Thomas JR, Shuman MA, Rosenberg S. Urokinase receptor antagonists inhibit angiogenesis and primary tumor growth in syngeneic mice. *Cancer Res* 1996; 56: 2428–33.
40. Ploug M, Østergaard S, Gårdsvoll H, Kovalski K, Holst-Hansen C, Holm A, Ossowski L, Danø K. Peptide-derived antagonists of the urokinase receptor. Affinity maturation by combinatorial chemistry, identification of functional epitopes, and inhibitory effect on cancer cell intravasation. *Biochemistry* 2001; 40: 12157–68.
41. Kuilman T, Michaloglou C, Vredeveld LC, Douma S, van Doorn R, Desmet CJ, Aarden LA, Mooi WJ, Peeper DS. Oncogene-induced senescence relayed by an interleukin-dependent inflammatory network. *Cell* 2008; 133: 1019–31.

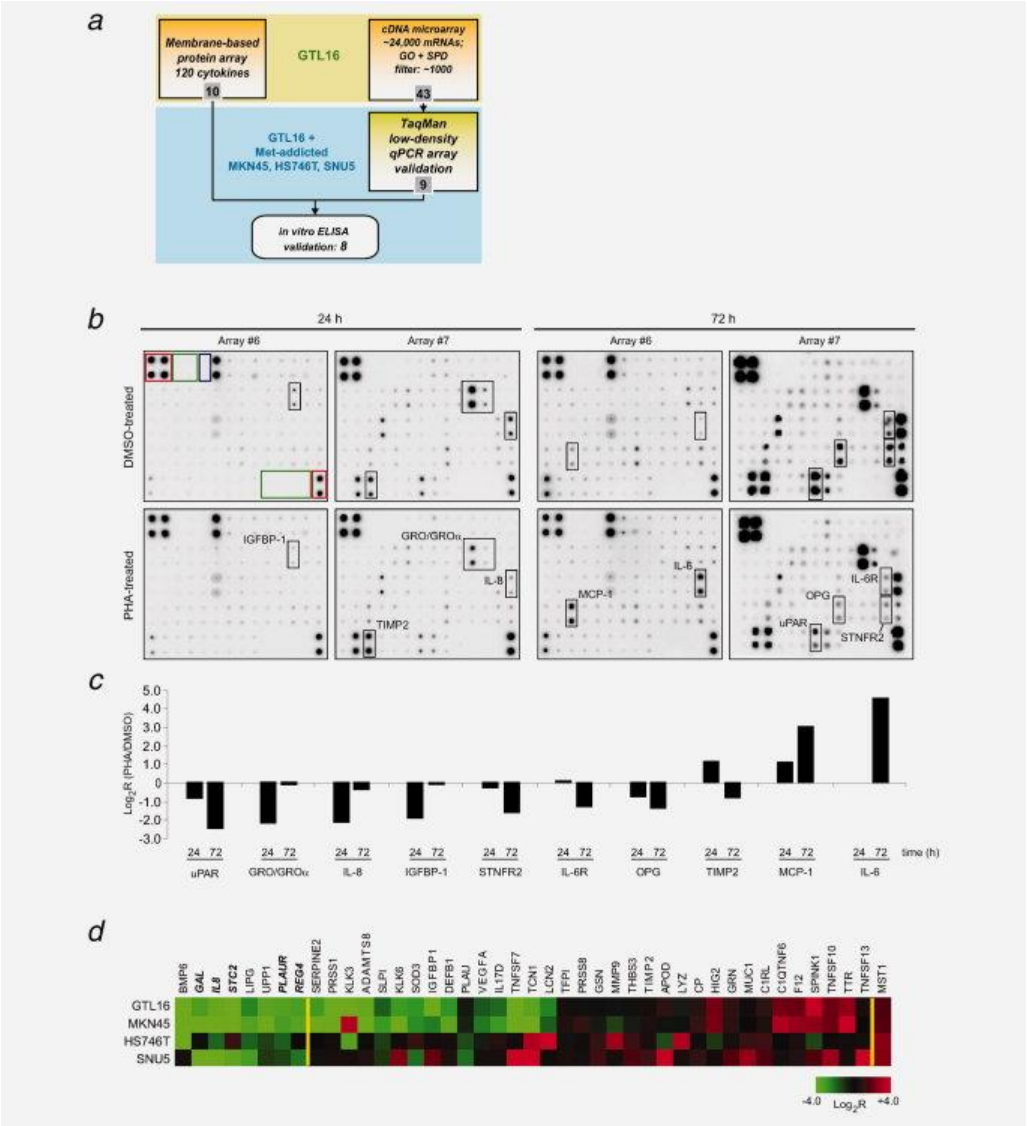

Figure 1. A multiplatform screen identifies candidate soluble biomarkers of Met inhibition in Met-addicted, drug-sensitive gastric carcinoma cell lines. (*a*) Flowchart of the experimental pipeline used for selection of candidate molecules; see text for details. (*b*) Representative images from the Cytokine Antibody Array; each membrane (#6 and #7) comprises a list of 60 different antibodies spotted in duplicate. Membranes were incubated with culture supernatants of GTL16 cells treated for 24 and 72 hr with DMSO (control) or the Met inhibitor PHA-665752 (PHA, 0.5 μM). Black squares identify the molecules of interest; red, green and dark blue squares indicate positive controls, blanks and negative controls, respectively. (*c*) Densitometric analysis of PHA-induced changes in the immunoreactivity of the soluble proteins highlighted in *a*; modulations are represented as $\log_2$ ratio between PHA- and DMSO-treated samples at 24 and 72 hr after PHA administration; ranking is from highest reduction to highest increase in protein production. (*d*) Heat map representing changes in the expression of 43 genes, based on TaqMan low-density qPCR arrays, in four Met-addicted gastric carcinoma cell lines (GTL16, MKN45, HS746T and SNU5) treated with DMSO (control) or 0.5 μM PHA for 24 hr; transcripts were extracted from a genome-wide expression dataset obtained in GTL16, using as selection criteria gene ontology annotations for secreted molecules and top-ranking candidates. Genes are ranked according to the average $\log_2$ ratio of transcript modulation across the four Met-addicted cell lines analyzed; yellow lines separate transcripts displaying average $\log_2$ ratio below (left) or above (right) ±2. Genes in bold italic were selected for further analysis.

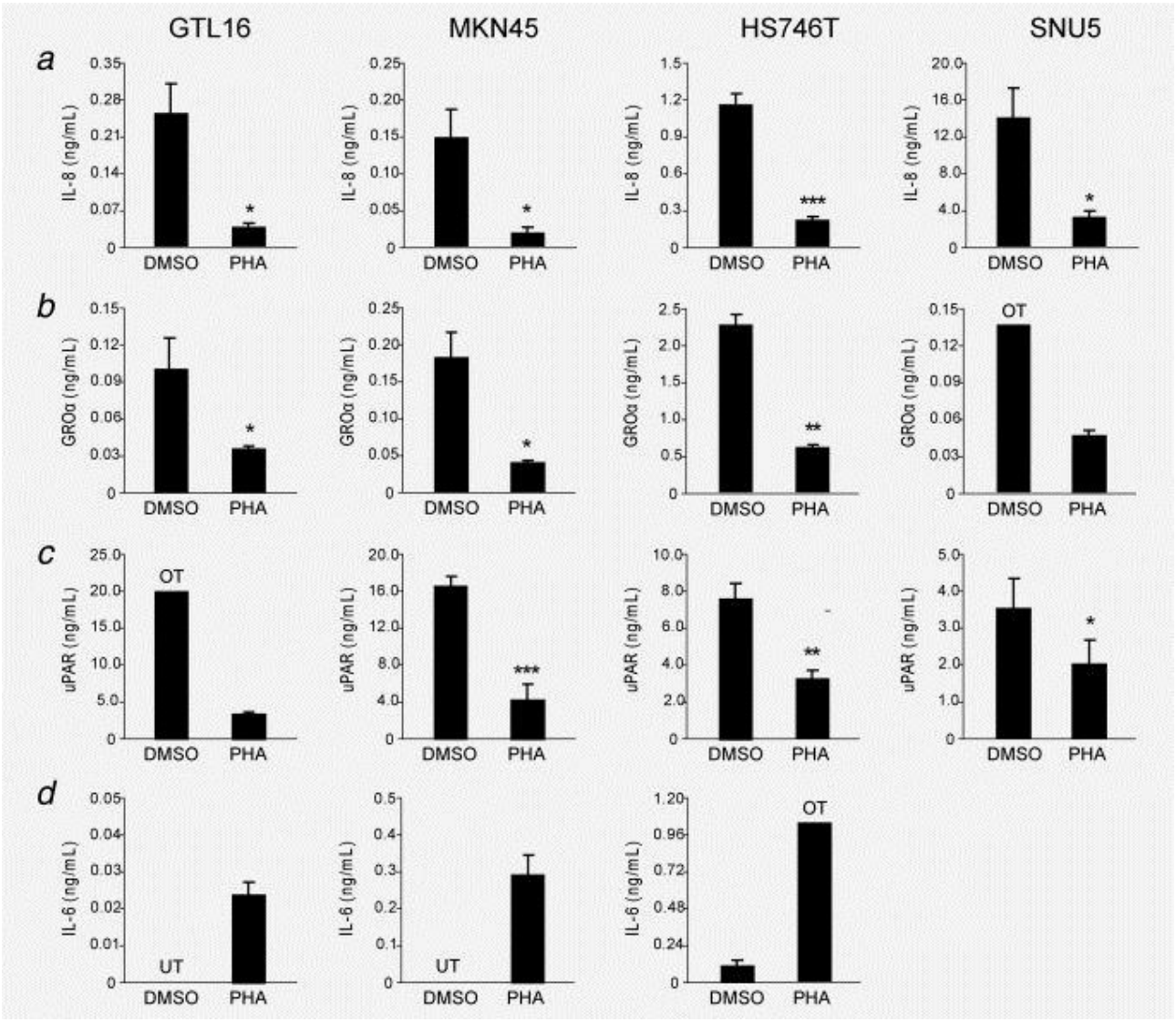

Figure 2. Met inhibition induces consistent changes in the secretion of IL-8, uPAR, GROα and IL-6 in a panel of Met-addicted cell lines. GTL16, MKN45, HS746 and SNU5 cells were treated with DMSO (control) or 0.5 μM PHA for 24 hr (IL-8, *a*, and GROα, *b*) or 72 hr (uPAR, *c*, and IL-6, *d*). Protein production was assayed by ELISA in culture supernatants, using calibration curves with purified proteins for analytical quantification. In culture supernatants of SNU5 cells, both basal and drug-modulated concentrations of IL-6 were below the detection threshold (data not shown). OT: overthreshold; UT: underthreshold. Data are the means ± SE (error bars) of one representative experiment performed in quadruplicate. *$p < 0.05$, **$p < 0.01$ and ***$p < 0.001$.

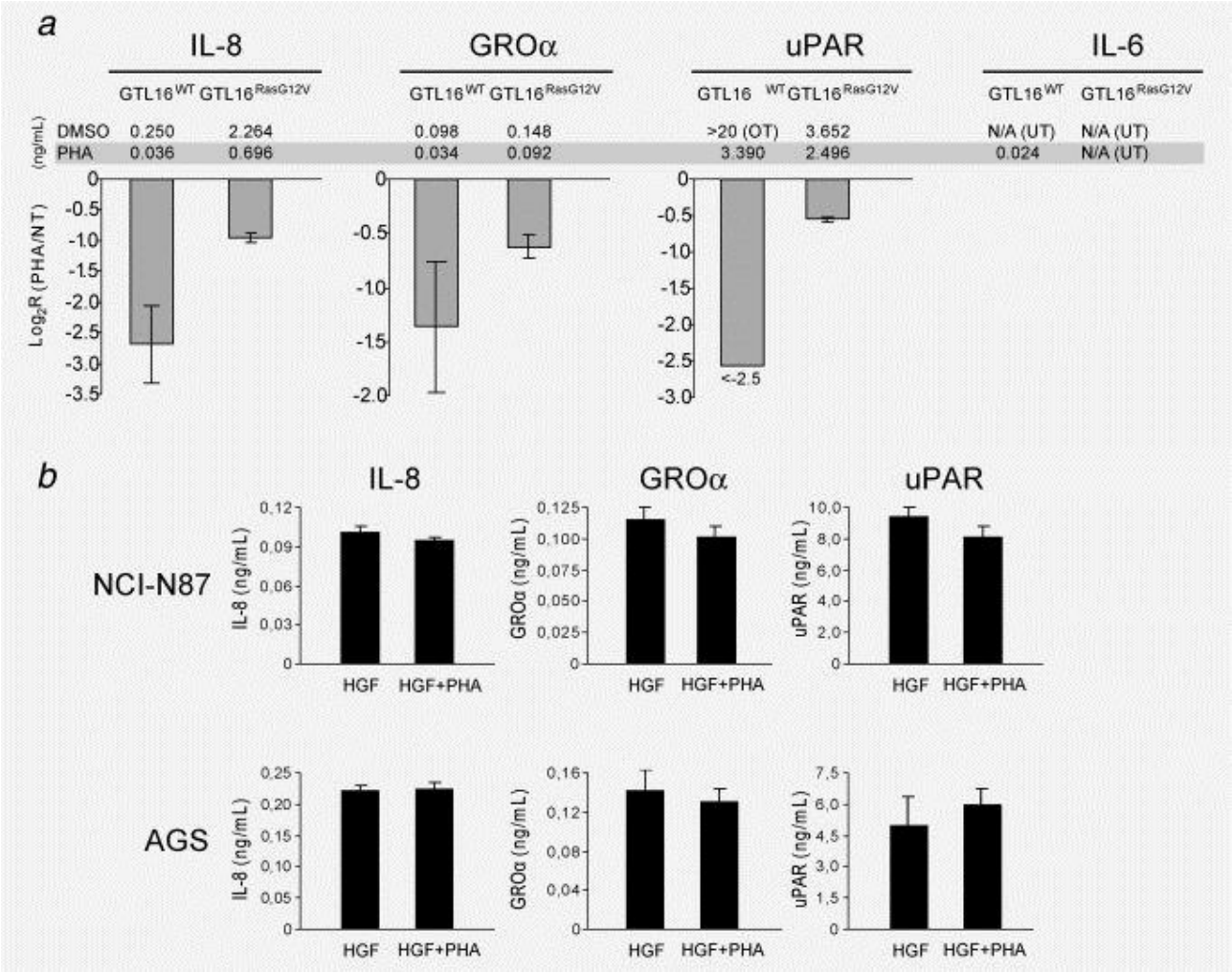

Figure 3. Modulation of IL-8, uPAR, GROα and IL-6 is blunted in cells that are biologically insensitive to Met inhibition. (*a*) Changes in the production of IL-8, GROα and uPAR are represented as $\log_2$ ratio of PHA- *versus* DMSO-treated samples in wild-type GTL16 cells ($GTL16^{WT}$) and in GTL16 cells expressing a constitutively active form of RAS ($GTL16^{RasG12V}$). Absolute quantities are also provided. In the case of IL-6, $\log_2$ ratios could not be calculated because production was under the detection threshold, with the exception of PHA-treated $GTL16^{WT}$ cells (see Fig. 2*d*). Data are the means ± SE (error bars) of two independent experiment performed in duplicate. OT: overthreshold; UT: underthreshold. (*b*) Met inhibition by PHA does not induce changes in the secretion of IL-8, GROα and uPAR in NCI-N87 and AGS gastric carcinoma cell lines cultured in the presence of HGF. In the case of IL-6, both basal and drug-modulated concentrations were below the detection threshold (data not shown). Data are the means ± SE (error bars) of one representative experiment performed in quadruplicate.

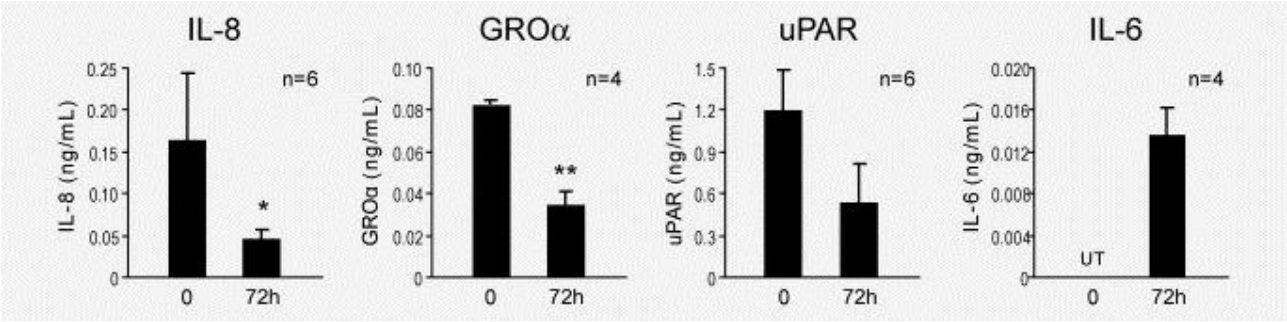

Figure 4. Pharmacologic inhibition of Met-addicted GTL16 xenografts induces consistent changes in plasma concentration of IL-8, GROα, uPAR and IL-6.

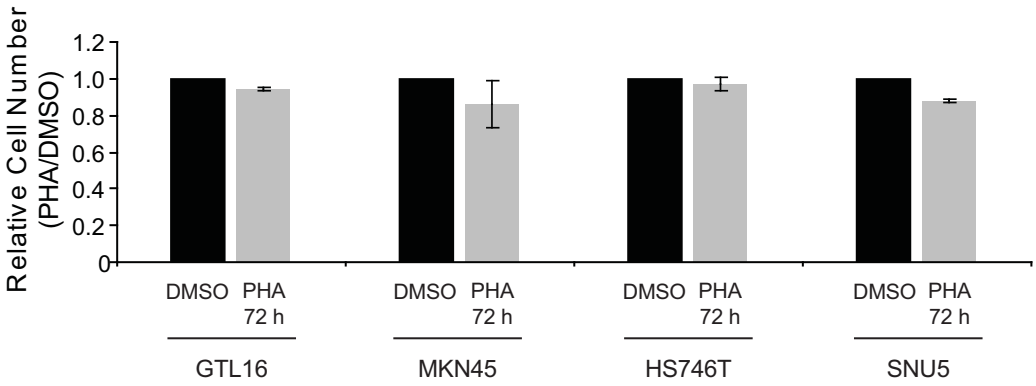

Figure S1. Met inhibition in overconfluent cells does not induce a significant reduction in cell counts. Represented histograms indicate that at the longer experimental timepoint (72 hours) overconfluent cells did not experience significant reduction in absolute cell numbers upon pharmacologic blockade of the Met receptor (0.5 μM PHA-665752). Hence, analytes' concentration in cell culture supernatants was not biased by the absolute number of cells secreting the biomarkers. Data are the means ± SD (error bars) of one representative experiment performed in quadruplicate.

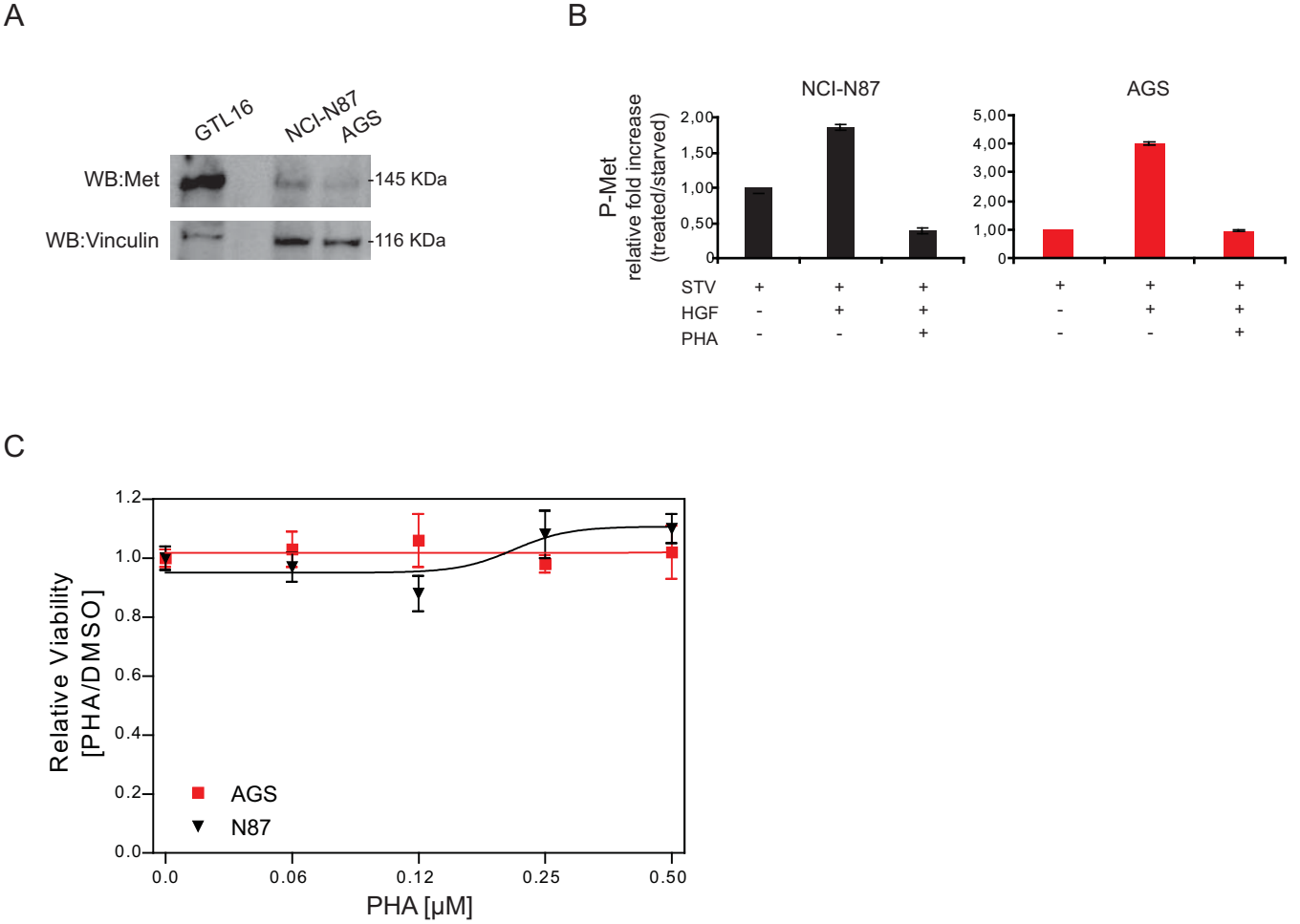

Figure S2. A, Met protein levels in total lysates of GTL16, NCI-N87 and AGS. Western blot analysis shows expression of Met protein in NCI-N87 and AGS cell lines, as compared to high-expressing GTL16 cells featuring amplification of the MET gene. **B,** Phospho-Met ELISA assay performed in NCI-N87 and AGS cells. Acute treatment (10 min) with HGF (50 ng/mL) induced phosphorylation of the Met receptor protein in both NCI-N87 and AGS cell lines, under starving conditions. The effect was completely abrogated when cells were concurrently exposed to the PHA-665752 anti-Met compound (0.5 uM). **C,** Dose-response curves of HGF-stimulated, PHA-inhibited NCI-N87 and AGS cells. NCI-N87 and AGS cell lines were cultured in the presence of 50 ng/mL HGF and subsequently inhibited with increasing doses of PHA-665752 for 72 hours. In both NCI-N87 and AGS, at all doses, treatment did not influence cell proliferation. Data are means ± SD (error bars) of one representative experiment performed in quadruplicate.

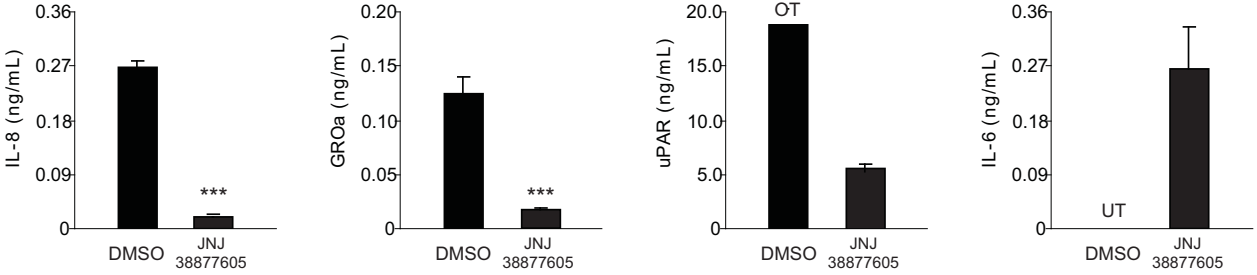

Figure S3. Inhibition of Met in GTL16 cells using the JNJ-38877605 compound induces changes in the secretion of IL-8, uPAR, GROa and IL-6 similar to those produced by PHA. Cells were treated with DMSO (control) or 0.5 μM JNJ for 24 hours (IL-8 and GROa) or 72 hours (uPAR and IL-6). Protein production was assayed by ELISA in culture supernatants, using calibration curves with purified proteins for analytical quantitation. OT, over threshold; UT, under threshold. Data are the means ± SE (error bars) of one representative experiment performed in quadruplicate. ***, $p<0.001$.

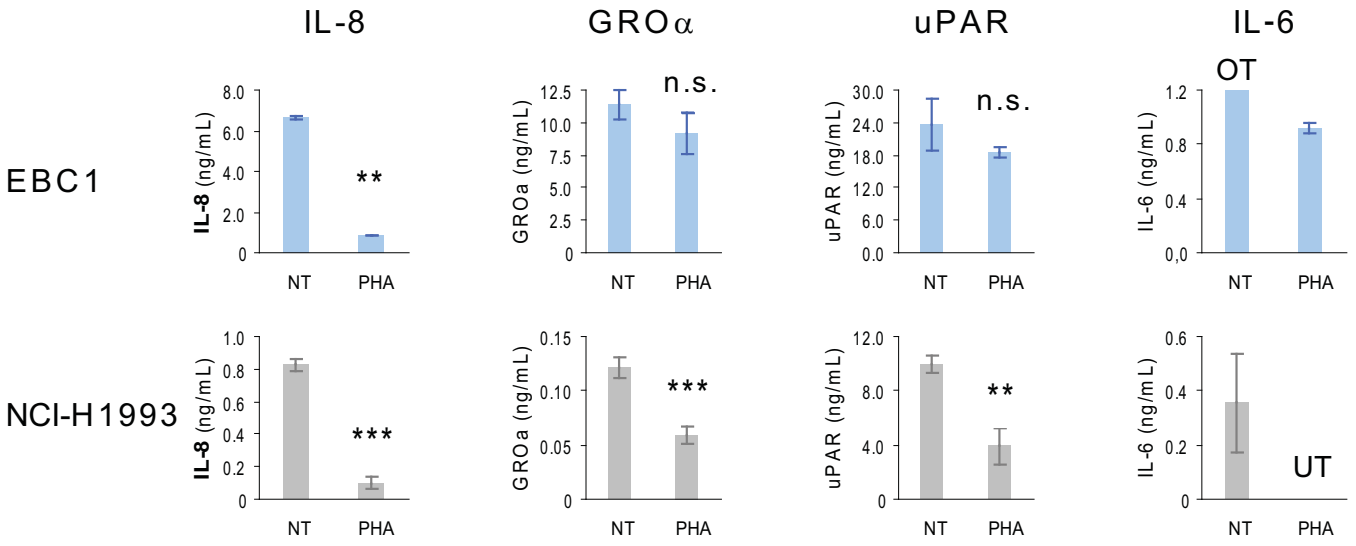

Figure S4. Met inhibition in EBC1 and NCI-H1993 lung cancer cell lines. Met inhibition with 0.5 μM PHA-665752 for 24 hours (IL-8 and GROα) or 72 hours (uPAR and IL-6) in the MET-amplified cell lines EBC1 and H1993 reduced the secretion of IL-8, GROα and uPAR, similar to that observed for MET-amplified gastric cancer cell lines. Of note, IL-6 showed an opposite behavior, featuring downmodulation instead of upregulation upon Met inhibition. Data are the means ± SE (error bars) of one representative experiment performed in quadruplicate.
**, $p<0.01$; ***, $p<0.001$.